Open Access Library Journal, 2014, 1, 1-14
Published Online June 2014 in OALib. http://www.oalib.com/journal
http://dx.doi.org/10.4236/oalib.1100504

OALib

Photocatalytic Destruction of Methylene Blue on Ag@TiO_2 with Core/Shell Structure

Yu-Wen Chen*, Der-Shing Lee

Department of Chemical and Material Engineering, Nanocatalysis Research Centre, National Central University, Jhong-Li, Taiwan
Email: *ywchen@cc.ncu.edu.tw

Received 13 April 2014; revised 18 May 2014; accepted 23 June 2014

Abstract

A series of Ag@TiO_2 catalysts with core-shell structure were successfully synthesized by a sol-gel method. The samples were prepared by a sol-gel method using silver nitrate, hydrazine, cetyltrimethylammonium bromide and titanium tetra-isopropoxide as the starting materials. The catalysts were characterized by ICP-MS, XRD, TEM, HRTEM and XPS. The results indicated that the silver core was in metallic state and the TiO_2 shell was in anatase state. The size of Ag nanoparticles in core was about 5 and 10 nm, and the shell size of titanium dioxide was 10 and 20 nm. The core was single crystalline Ag nanoparticle and the shell was made up of many TiO_2 nanoparticles. The photocatalytic activity of Ag@TiO_2 was much higher than that of bare TiO_2. Large amounts of hydroxyl groups were present on the surface of TiO_2. The catalysts which were treated by hydrothermal method had the higher lattice oxide percentage and higher photocatalytic activities. The core-shell structure can prevent Ag from aggregation.

Keywords

Green Catalyst, Photocatalyst Titania, Silver

1. Introduction

Titanium dioxide is the most successful photocatalyst that has attracted the interest of researchers for many decades because of its chemical stability, low cost, excellent degradation for organic pollutants and nontoxic property [1]-[4]. Hetergeneous photocatalytic oxidation is a promising technique for the complete oxidation of dilute pollutants in waste gas stream. The organics can be oxidized to H_2O and CO_2 at room temperature with TiO_2 catalyst in air when illuminated with UV light or near UV light. The UV light excites electrons from the valen-

*Corresponding author.

How to cite this paper: Chen, Y.-W. and Lee, D.-S. (2014) Photocatalytic Destruction of Methylene Blue on Ag@TiO_2 with Core/Shell Structure. *Open Access Library Journal*, **1**: e504. http://dx.doi.org/10.4236/oalib.1100504

ceb and into the conduction band, which results in the migration of electron-hole pairs to the surface and initiate redox reactions with adsorbed organics [5]-[13]. Noble metal deposition method was widely used to enhance the photocatalytic activity of TiO_2. Pt and Ag deposited on TiO_2 film using chemical vapordeposition method have been studied by many researchers and Ag/TiO_2 showed a better photocatalytic activity than other catalysts [9] [14]-[17]. Noblemetal nanoparticles such as silver and gold are known to exhibit size-dependent specific optical, electric and catalytic [18] [19] properties [20], and surface plasmon absorption [21].

The literature reports showed that noble metals doped on TiO_2 surface could enhance the photocatalytic activity, by acting as an electron trap; thereby promoting interfacial charge transfer processes in the composite system [22]-[25]. However, in a long run, there is a possibility of dissolution, corrosion and reaction of metals during the photocatalytic reaction, which limits the efficacy of photocatalysts. An effective way to solve these short comings is to use a core/shell structure in which the noble metal nanoparticles perform as cores, and TiO_2 acts as a shell [26]-[28]. Wang *et al*. [28] reported a sol-gel method to prepare $Ag@TiO_2$ which is active for destruction of methylene blue (MB). However, the effects of Ag loadings and hydrothermal treatment on the photocatalytic activity of TiO_2 have not yet examined in detail.

The preparation parameters such as pH, heating time, and heating temperature plays a vital role in the synthesis of $Ag@TiO_2$ by a sol-gel titanium dioxide sol. The preparation by chemical reduction of noble metal salt also needs to control the precursor concentration. Preparation conditions and concentration of reducing agent to control the size of noble metal particles in the mixture after the reaction should consider the temperature and heating time to have core-shell structure [29]-[33]. Hirakawa and Kamat [20] have studied charge separation and catalytic activity of $Ag@TiO_2$ in detail. However, they did not get high crystallinity of TiO_2 shell. It is important to have anatase TiO_2. In this study, we used hydrothermal method to obtain anatase TiO_2 instead of using high temperature treatment.

Dye pollutants were discharged from textile industry which is one of the reasons for environment contamination [34] [35]. The waste pollutants within water in the ecosystem perturbed the aquatic life because of eutrophication. Methylene blue was atypical dye pollutant in textile industry. The structure of MB is shown in **Figure 1**.

In this study, $Ag@TiO_2$ nanoparticles were synthesized by a sol-gel method and treated by hydrothermal method to form a core-shell structure. The aim of this study was to develop an optimum method to prepare core-shell structure which has a high activity to destruct MB under UV light irradiation. The photocatalytic activity of these materials was treated by the photodegradation of methylene blue in water.

2. Experimental Procedures

2.1. Material

The precursors for silver and titania are silver nitrate (Sigma-Aldrich) and titaniumtetra-isopropoxide (TTIP; Sigma-Aldrich), respectively. The reducing agent used in the preparation method is hydrazine solution (Sigma-Aldrich). Cetyltrimethyl ammoniumbromide (CTAB; Sigma-Aldrich) was used as the protective agent, while ethanol (JT Baker) was used as the solvent for TTIP. All reagents used in this study were analytical grade.

2.2. Synthesis of $Ag@TiO_2$

At first, different amounts of 100 mM aqueous hydrazine solution were added into 1 mM CTAB solution. Preparation of silver clusters was by reduction of silvernitrate. Different amounts of 50 mM $AgNO_3$ were added into the above mixture. The final composite was stirred for 30 min at room temperature to reach high dispersive state in this solution. The TTIP was dropped into ethanol and then the solution was slowly added to the Ag nanoparticle suspension under stirring for several minutes to yield a suspension of silver-titania composite nanoparticles.

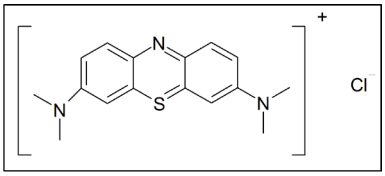

Figure 1. Structure of methylene blue (MB).

The excess solvent was removed by rotary evaporation until the $Ag@TiO_2$ powder was produced. The mixture was divided into two parts. One was treated by hydrothermal method in a Teflon-lined autoclave at 180˚C for 12 h, and the other one was stayed at room temperature, instead of hydrothermal condition. The products were recovered by centrifugation, and then washed with distilled water to remove residues and finally dried at 50˚C in an oven overnight. The powder was grinded and $Ag@TiO_2$ was obtained. The molar ratios of the chemicals were based on TTIP, and the TTIP concentration to prepare $Ag@TiO_2$ nanoparticles as listed in **Table 1**; in which HT stands for the catalyst treated by hydrothermal method. The volume of ethanol was changed to get different concentrations of TTIP.

2.3. Characterization

Inductively-coupled plasma-mass spectrometry (ICP-MS), X-ray diffraction (XRD), transmission electron microscopy (TEM), selective area electron diffraction(SAED), high resolution transmission electron microscopy (HR-TEM), and X-rayphotoelectron spectroscopy (XPS) were used to characterize the $Ag@TiO_2$ samples. UV-Vis spectroscopy (UV-Vis) was used to measure the methylene blue (MB) concentrations of the samples before and after reaction.

2.3.1. ICP-MS

The real silver content was analyzed by ICP-MS (PE-SCIEX ELAN 6100DRC). A CEM MDS-2000 (CEM, Matthews, NC, USA) microwave apparatus equipped with Teflon vessels was used to digest the powder samples.

2.3.2. XRD

XRD experiments were performed using a Siemens D5000 powder diffractometer using CuKα1 radiation (1.5405 Å) at a voltage and current of 40 kV and 30 mA, respectively. The sample was scanned over the range $2\theta = 20^\circ - 80^\circ$ at a rate of 0.05˚/min to identify the crystalline structure. Samples for XRD were prepared as thin layers on a sample holder.

2.3.3. TEM and HRTEM

The morphologies and particle sizes of the samples were determined by TEM on a JEM-2000 EX II operated at 160 kV and HRTEM on a JEOL JEM-2100 operated at 160 kV. Initially, a small amount of sample was placed into the sample tube filled with a 95% methanol solution and after agitating under ultrasonic environment for 10 min, three drops of the dispersed slurry was dipped onto a carbon-coated copper mesh (200#) (Ted Pella Inc., CA, USA), and dried in the vacuum oven at 25˚C for 1 day. Images were recorded digitally with a Gatan slow scan camera (GIF). Based on the several images of TEM or HRTEM, more than 100 particles were counted and the sized is tribution graph was made.

2.3.4. XPS

The XPS spectra were recorded with a Thermo VG Scientific Sigma Probspectrometer. The XPS spectra were collected using Al Kα radiation at a voltage and current of 20 kV and 30 mA, respectively. The base pressure in the analyzing chamber was maintained in the order of 10^{-9} torr. The spectrometer was operated at 23.5 eV pass energy and the binding energy was corrected by contaminant carbon (C 1s = 284.6 eV) in order to facilitate the comparisons of the values among the catalysts and the standard compounds. Peak fitting was done using XPSPEAK 4.1 with Shirley background and 30:70 Lorentzian/Gaussian convolution product shapes.

2.4. Degradation of Methylene Blue

0.02 g $Ag@TiO_2$ samples were added into 200 mL 10 ppm MB solution. Reactions were carried out in the circular container by top scattering of UV light. The light source was from two 1.5 W UVC lamps (254 nm; Germicidal lamp from Sankyo Denki Co., Ltd.). At given time intervals, the analytical samples were taken from the mixture and immediately centrifuged and then filtered through a 0.22-μm Milliporefilter to remove the particles. The concentration of MB blue in water was determined by a UV-Vis spectrophotometer (Varian Cary 300). Liquid samples were loaded in aquartz cell, and the spectra were collected against barium sulfate standard. There action setup is shown in **Figure 2**. The photodegradation efficiency (X) can be calculated as following equations:

Table 1. Molar ratios of precursors used in the preparation of various Ag@TiO_2 catalysts.

Catalyst	$AgNO_3$	N_2H_5OH	CTAB	TTIP	Ethanol	Conc. of TTIP
A	0.01	0.02	0.004	1	171.12	100 mM
B	0.005	0.01	0.004	1	171.12	100 mM
C	0.005	0.01	0.004	1	102.67	167 mM
D	0.005	0.01	0.004	1	136.9	125 mM
HT-A	0.01	0.02	0.004	1	171.12	100 mM
HT-B	0.005	0.01	0.004	1	171.12	100 mM
HT-C	0.005	0.01	0.004	1	102.67	167 mM
HT-D	0.005	0.01	0.004	1	136.9	125 mM

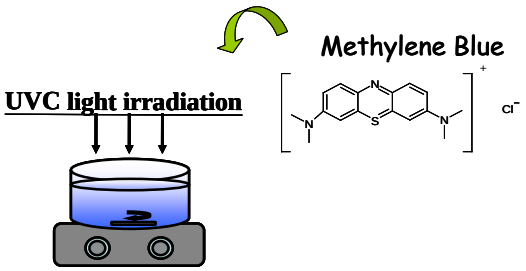

Figure 2. Reaction setup for MB degradation.

$$X = (A_0 - A)/A \quad (1)$$

$$A = A_0 - (A_b - A_s) \quad (2)$$

where A_0 is the initial absorbance of reference MB solution and A is the revised absorption considering MB after photo irradiation. Equation (2) was used for elimination of blank effect and correction the consequence of photodecomposition. A_b is absorbance of blank and A_s is the absorbance of sample.

3. Results and Discussion

Metal core-oxide shell structures were prepared by one pot synthesis that involved reduction of metal ions and hydrolysis of TTIP in methanol. Ag^+ ions were reduced by hydrazine, followed by the slow hydrolysis of TTIP to form a shell around the metal core. As Ag^+ ions are reduced by hydrazine to form small metal particles, they quickly interact with the CTAB. The condensation polymerization of TTIP slowly progresses on the surface of Ag particles to yield TiO_2 shell.

The stability of Ag@TiO_2 was confirmed by checking the stability in an acidic solution (HNO_3). The Ag cluster was readily dissolved in HNO_3 acidic solution (pH = 2). Ag@TiO_2 was quite stable in HNO_3 solution. The stability test in acidic solution confirms that the TiO_2 shell on the Ag core was uniform and provided the protection against acid induced corrosion. The samples were also tested by high temperature calcinations. Ag particle size did not increase, indicating that Ag core was protected and constrained by TiO_2 shell.

3.1. ICP-MS Results

Ag loading in the sample was measured by ICP-MS. The nominal Ag loadings of the samples were 0.67 wt% and 1.33 wt%, respectively. The real Ag loadings in the samples are tabulated in **Table 2**. The results show that only 60% - 80% of the original Ag was deposited in the sample, *i.e.*, 20% - 40% silver cations in the starting material were not deposited in the solid product. All Ti cations were converted to TiO_2 because TTIP is very easy to react with water.

Table 2. Actual silver loading on titania based on ICP-MS results.

Catalysts	Nominal (wt%)	Actual (wt%)
	Ag	Ag
A	1.33	1.10
B	0.67	0.411
C	0.67	0.480
D	0.67	0.456
HT-A	1.33	1.33
HT-B	0.67	0.66
HT-C	0.67	0.517
HT-D	0.67	0.483

3.2. XRD

Figure 3 shows the XRD patterns of all samples. It is obvious that after hydrothermal treatment, the crystallinity of the sample increased significantly, as expected. The samples after hydrothermal treatment exhibited four characteristic peaks for the (101), (004), (200), and (105) planes of anatase TiO_2 at 2θ = 25.3˚, 37.8˚, 48.1˚ and 53.9˚. No rutile phase was observed. The peak was not very intense, inferring that the crystallite size was small. This matches our objective to make nanocrystallite. The crystallite size of TiO_2, calculated by the Bragg's equation, was 6 nm. The XRD patterns of the samples also exhibited three characteristic peaks for the (111), (200), and (220) planes of face-centered cubic (fcc) Ag at 2θ = 38.1˚, 44.3˚ and 64.4˚. Nopeak corresponding to AgO was observed. Because the Ag particle size was small, the peak was almost invisible. The crystallite size of Ag was only about 3 - 4 nm. The color of the sample became darker when the sample was treated by hydrothermal condition. It was attributed to crystallization of Ag metal.

3.3. TEM/HR-TEM

The core/shell structure of materials such as shape, particle size and size distribution were analyzed by TEM. The TEM photographs shown in **Figure 4** show the core/shell morphology of the samples. The dark spot is Ag. The Ag particles were surrounded by TiO_2 shell. The size of Ag core was about 3 - 5 nm, and the shell thickness of TiO_2 was 5 - 10 nm. The core was a crystalline Ag nanoparticle and the shell was made up of many TiO_2 nanoparticles. It should be noted that it was easier to form $Ag@SiO_2$ than $Ag@TiO_2$, because TTIP was too reactive with water.

Figure 5 shows the typical HR-TEM image of the $Ag@TiO_2$ (HT-A sample). The value in the parentheses is the distance of lattice in database, and the other number is the distance of lattice in the photograph. The Ag particle was very small. The HR-TEM photographs also shows that the silver was (111) plane in Miller index and the titanium dioxide was anatase structure of (101) plane in Miller index. No other plane was found.

Figure 6 shows the diffraction images of the sample HT-C. The result clearly shows that Ag and TiO_2 are well-crystalline after hydrothermal treatment, inaccordance with XRD results. The other samples also showed the same results.

3.4. XPS

Figure 7 shows the XPS spectra of Ag 3d in all samples. Each silver species shows two peaks, which was assigned to Ag $3d_{5/2}$ and Ag $3d_{3/2}$. The peaks for bulk metallic silver are centered at 368.2 eV and 374.2 eV, while the peaks for Ag_2O are 367.8 eV and 373.8 eV and for AgO are 367.4 eV and 373.4 eV [8]. The intensity of XPS peak for Ag increased with increasing Ag loading, as expected. The distributions of these peaks are sharp and with symmetry, inferring that there was only one chemical state in Ag. Ag is in metallic state. The binding energies of Ag shifted to lower energy, indicating that Ag particles had strong interaction with TiO_2, and the excited electrons in TiO_2 transferred to Ag particles. The catalysts treated by hydrothermal method shifted less than those without hydrothermal treatment.

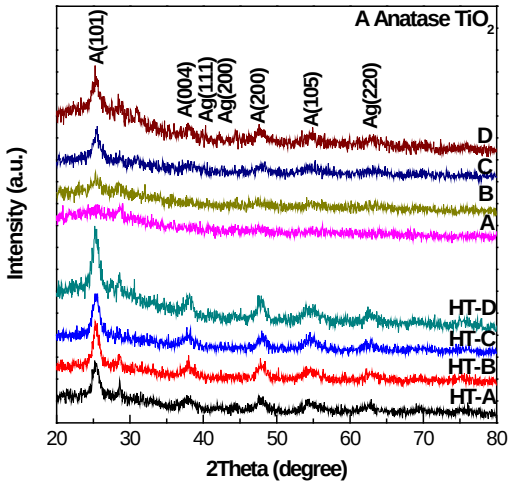

Figure 3. XRD patterns of various Ag@TiO_2 samples.

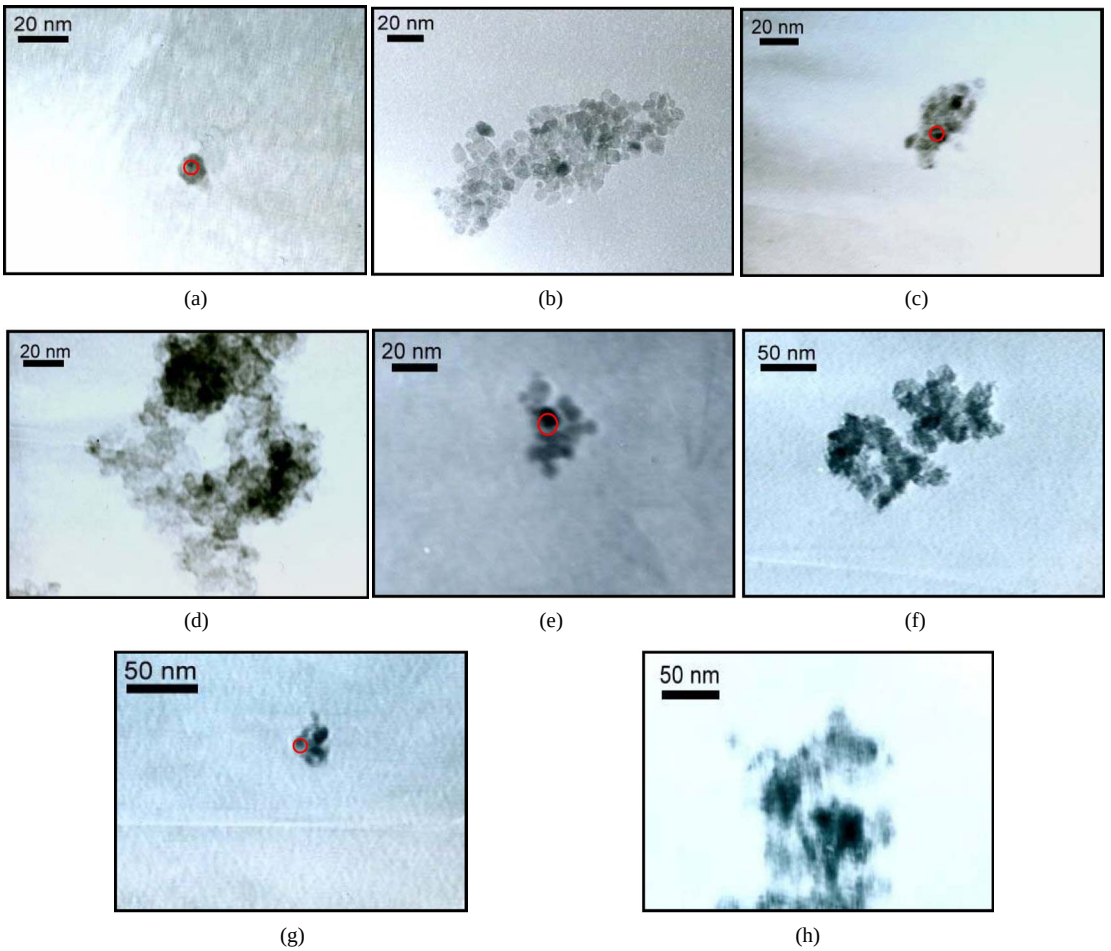

Figure 4. TEM images of Ag@TiO_2, (a) HT-A, (b) A, (c) HT-B, (d) B, (e) HT-C, (f) C, (g) HT-D, (h) D. HT stands for the catalyst treated by hydrothermal method.

The biding energies of Ti^{4+} $2p_{1/2}$ and Ti^{4+} $2p_{3/2}$ are centered at 458.6 eV and 464.4 eV, respectively [36] [37]. The spectra of Ti 2p region of the samples are shown in **Figure 8**. Because these peaks are sharp and with symmetry, one can conclude that there is only one chemical state in Ti. The results show that Ti in Ag@TiO_2 was in

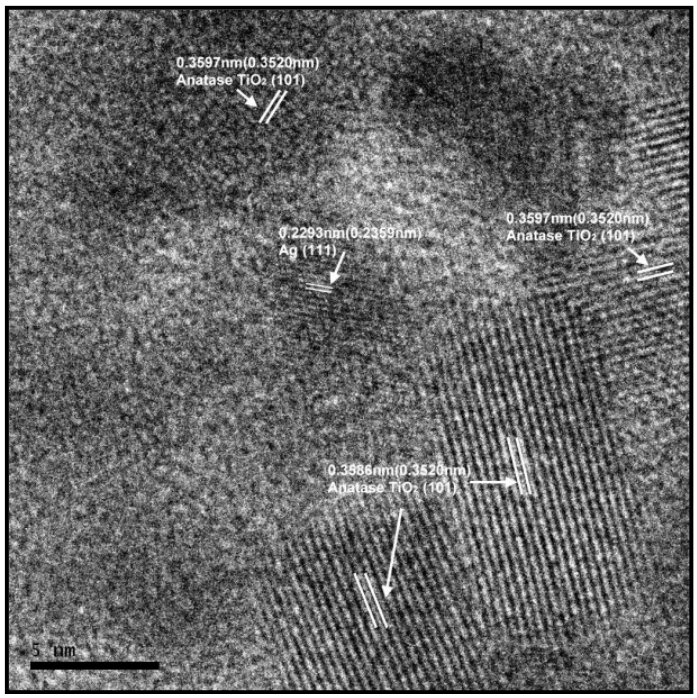

Figure 5. HR-TEM image of Ag@TiO_2 after hydrothermal treatment (HT-A).

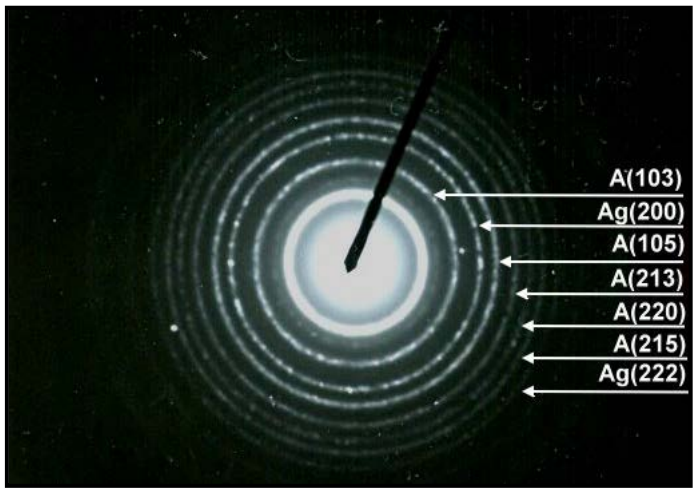

Figure 6. Diffraction image of the sample HT-C.

Ti^{4+} valence state. In other words, only anatase TiO_2 was present and Ag did not change the electronic state of Ti. Since very small amount of Ag was used, therefore it is difficult to change the binding energy of Ti.

Two peaks are evident in O 1s core level spectra of the samples as shown in **Figure 9**. According to the literature, the binding energies of O^{2-} and OH^- are centered at 530.2 eV and 532.0 eV, respectively [37]. The peaks of O^{2-} and OH^- all shifted to lower binging energy level at 530.1 eV and 531.7 eV, respectively. The atomic percentages of O^{2-} and OH^- in Ag@TiO_2 were calculated from XPS peak areas and are tabulated in the **Table 3**. The atomic ratio of O^{2-} to OH^- in Ag@TiO_2 was around 4:1. The catalysts which were treated by hydrothermal method had the higher lattice oxide percentage, indicating that they had higher crystallinity. The results also demonstrated that large amount of hydroxyl groups were present on the surface of the samples. Under UV irradiation, the surface hydroxyl groups were converted to hydroxyl radicals, which are crucial for the photocatalytic activity.

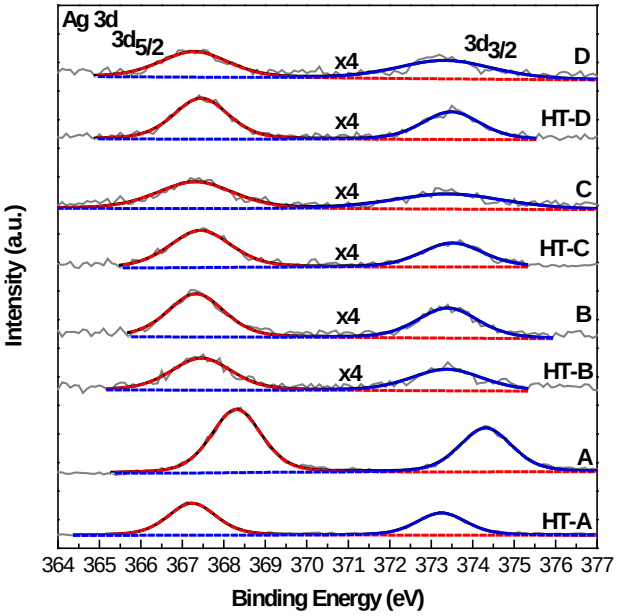

Figure 7. XPS analysis for Ag 3d.

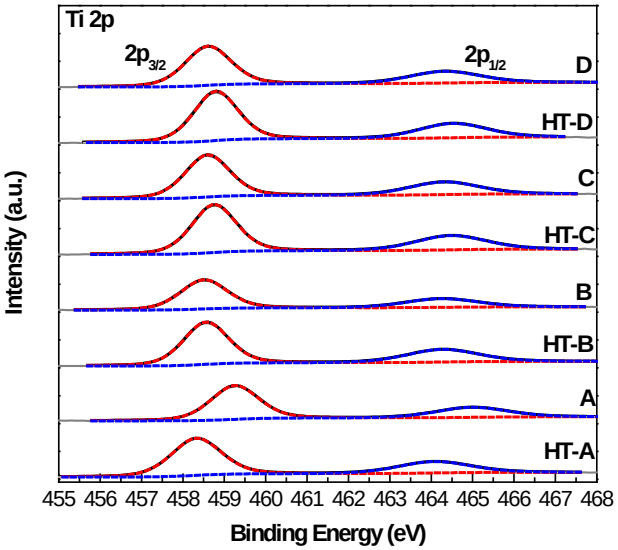

Figure 8. XPS analysis for Ti 2p.

The splitting between Ti $2p_{1/2}$ and Ti $2p_{3/2}$ was 5.8 eV, indicating Ti existed as Ti^{4+} in the as-prepared TiO_2 and Ag/TiO_2 film [36]. No peaks due to Ti^{3+} were observed, indicating that TiO_2 was not reduced during UV irradiation process. As expected, TiO_2 was very stable in reaction. The deconvoluted O 1s spectra of TiO_2 and Ag/TiO_2 are presented in **Figure 9**. The characteristic O 1s peak located at 530.6 eV was ascribed to the lattice O^{2-} of TiO_2. The assignment of the peak at 532.3 eV was ambiguous. It has been attributed to adsorbed oxygen, surface oxygen vacancies, hydroxyl group, and absorbed water [38]-[45]. Here, we assigned this peak to hydroxyl group existed on the surface of the TiO_2 and Ag/TiO_2 film. The ratio of peak area at 532.3 eV versus total O 1s peak area could express the relative content of hydroxyl group. The corresponding ratios of the two films are listed in **Table 1**. It shows that the content of the surface hydroxyl group for Ag/TiO_2 film was higher than that of bare TiO_2.

The explanation for the different amounts of surface hydroxyl groups was as following. Under UV irradiation, the electrons in the valence band (VB) of TiO_2 could be promoted to the conduction band (CB). Therefore the

Table 3. Binding energies of various chemical species present in Ag@TiO_2 and the percentage of different oxygen species.

Catalysts	Ag 3d		Ti 2p		O 1s			
	$3d_{5/2}$ (eV)	$3d_{3/2}$ (eV)	$2p_{3/2}$ (eV)	$2p_{1/2}$ (eV)	OH^- (eV)	%	O^{2-} (eV)	%
HT-A	367.23	373.25	464.08	458.33	531.57	33.35%	530.16	66.65%
A	368.30	374.31	464.97	459.25	532.23	34.65%	530.65	65.35%
HT-B	367.46	373.38	464.27	458.56	531.36	20.34%	530.04	79.66%
B	367.33	373.40	464.24	458.51	531.67	30.40%	530.17	69.60%
HT-C	367.44	373.50	464.47	458.75	531.66	19.94%	520.14	80.06%
C	367.31	373.41	464.30	458.59	531.71	20.67%	530.17	79.33%
HT-D	367.45	373.48	464.52	458.80	531.59	18.75%	530.18	81.25%
D	367.29	373.34	464.32	458.61	531.61	31.79%	529.96	68.21%

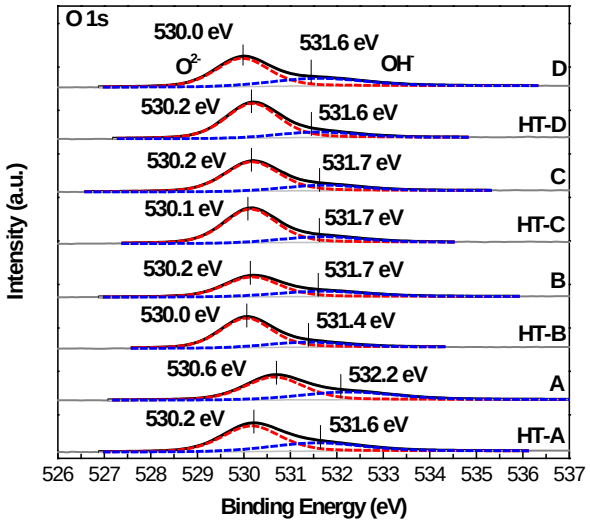

Figure 9. XPS analysis for O 1s.

holes were formed in the valence band. The holes were assumed to be trapped by lattice oxygen atoms on the surface of the TiO_2 film [38]-[47]. The trapped hole was thought to weaken the bond between the titanium atom and the lattice oxygen atom. As a result, such oxygen atom was liberated to create oxygen vacancies [46]-[49]. After the UV irradiation of the catalyst, the TiO_2 and Ag@TiO_2 films became super-hydrophilic. Water molecules could be absorbed onto the samples easily. The absorbed water molecules occupied the vacancy sites to reduce the surface energy even if it was present in almost negligible amounts. There was a strong interaction between the vacant sites and the absorbed water molecules, resulted in releasing a proton to a nearby oxygen atom and formed two hydroxyl groups [50]-[55].

3.5. Photoactivity Test

The degradation curves of MB on Ag@TiO_2 nanoparticles are shown in **Figure 10**. All the Ag@TiO_2 samples were more active than the bare TiO_2, indicating that Ag is a good cocatalyst. The presence of Ag could suppress electron-hole recombination, thereby increasing the photocatalytic activity. Among these samples, all of Ag@TiO_2 catalysts had a higher photodegradation rate of MB than bare TiO_2. It can be contributed to a Schottky energy barrier formed by the combination of Ag clusters and TiO_2 shells. The interface can attract light-induced electrons from the semiconductor TiO_2 to reduce electron-hole recombination. Ag core should be reduced to Ag metal because AgO cannot serve as a Schottky energy barrier [56]-[60].

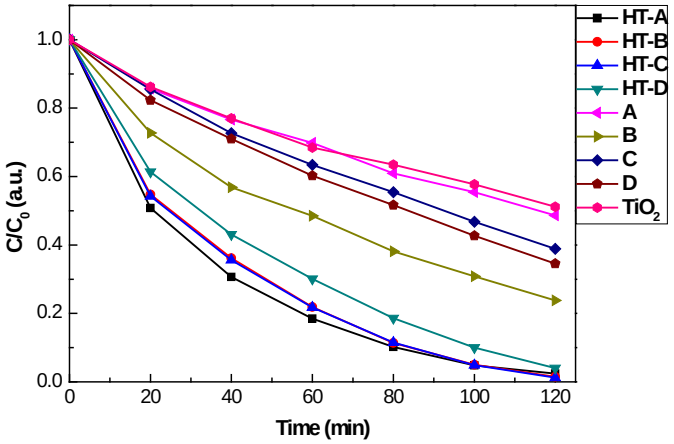

Figure 10. The degradation of MB on $Ag@TiO_2$ and TiO_2. (The reactants were 0.02 g Ag/TiO_2 with 200 ml 10 ppm MB solution).

For explain of this results, silver and TiO_2 have different work functions, ($\Phi_{TiO_2} = 4.2$ eV, $\Phi_{Ag} = 4.6$ eV). When silver comes in contact with TiO_2, electrons will transfer from TiO_2 to silver. These electrons transferred to silver and loaded on the surface of silver will be scavenged by the electron acceptor, thus decreases there combination between electron and hole and silver atoms act as electron traps. It is well known that the electron-hole recombination is the main reason for low efficiency of TiO_2 photocatalysis [1]-[6]. Therefore, the existence of silver atom in $Ag@TiO_2$ can help more holes to transport to the surface and enhance the photocatalytic activity.

The samples treated by hydrothermal method had the higher activities than those without hydrothermal treatment, as shown in **Figure 11**. It is attributed to the high crystallinity of TiO_2. It is well-known that anatase TiO_2 is a semiconductor and it has photocatalytic activity. Amorphous TiO_2 is an insulator, and does not have photocatalytic activity.

As shown in **Figure 7**, the Ag particles inside the TiO_2 shell could act as electron-hole separation centers. The photo-generated electrons transferred from the TiO_2 conduction band to metallic silver particles inside TiO_2. This process is thermodynamically possible because the Fermi level of TiO_2 is higher than that of silver metals. The Schottky barrier is formed at the Ag-TiO_2 contact region, which improved the charge separation and thus retarded the recombination of the photo-generated electrons and photo-generated holes. The photo-generated electrons accumulated on the surface of Ag have good fluidity and can be transferred to oxygen molecules, which is absorbed on the surface of Ag. As shown in **Figure 7**, the oxygen molecules could easily obtain the electrons to form H_2O_2, HO_2^- and O_2^- [56]-[59]. These active species significantly promoted the photocatalytic oxidation process. Furthermore, the holes were accumulated at the valence band. The water molecules adsorbed on the surface of TiO_2 could interact with the holes, leading to the production of surface hydroxyl radical •OH, which is responsible for the oxidation decomposition of MB. This also favors the photocatalytic process of $Ag@TiO_2$.

The relative amount of surface hydroxyl group of the sample was very crucial for the photocatalytic properties. This is another reason for the high photocatalytic activity of $Ag@TiO_2$. During the photocatalytic process, the hydroxyl groups on the surface is active in the oxidation process of organics by capturing a hole resulted information of hydroxyl radicals [60]-[63]. The increase in the content of hydroxyl groups on the surface of TiO_2 enhanced the photocatalytic activity.

4. Conclusion

A series of $Ag@TiO_2$ samples with core-shell structure were successfully synthesized by sol-gel method. The results indicated that silver core was in metallicstate and the TiO_2 shell was in anatase state. The size of Ag nanoparticles in core was about 5 and 10 nm, and the shell size of titanium dioxide was 10 and 20 nm. The core was single crystalline Ag nanoparticle and the shell was made up of many TiO_2 nanoparticles. The photocatalytic activity of Ag/TiO_2 was much higher than that of TiO_2. The atomic ratio of O_2^- to OH^- in $Ag@TiO_2$ was 4:1. The catalysts which were treated by hydrothermal method had the higher lattice oxide percentage and higher

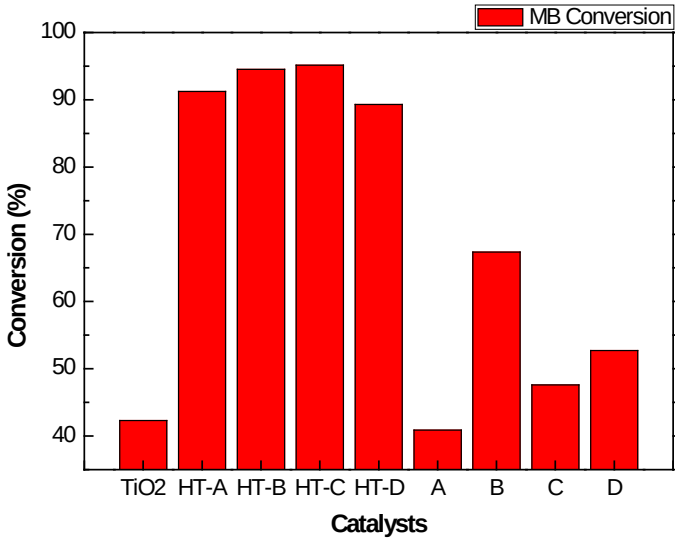

Figure 11. The conversions of methylene blue on Ag@TiO_2 and TiO_2 after 100 min reaction time with UV light irradiation.

photocatalytic activities, indicating that the crystallinity of the TiO_2 structure affected the band gap. There is an optimal Ag loading to have the highest activity. The core-shell structure can prevent Ag from aggregation. Compared to the pure TiO_2, Ag@TiO_2 showed a significant increase in photocatalytic activity on degradation of methylene blue. XPS studies showed that the amount of the surface hydroxyl groups on Ag@TiO_2 was higher than that of TiO_2 film. Under UV irradiation, the surface hydroxyl groups were converted to hydroxyl radicals, which were crucial for the photo-catalytic activity. The doping of Ag inside TiO_2 shell retarded there combination of the photo-generated electrons and holes, which favored the formation of surface hydroxyl groups. Furthermore, the electrons trapped by Ag particles could react with oxygen to form the active species for the photocatalytic process. The preparation method made Ag close contact with TiO_2, which could guarantee the transfer of the photo-generated electrons from conduction band of TiO_2 to Ag nanoparticles. Consequently, the presence of Ag inside TiO_2 shell could enhance the photocatalytic activity of TiO_2. Although the Ag loading was very low (<1 wt%), the Ag@TiO_2 showed excellent photocatalytic activity.

Acknowledgements

This research was supported by the National Science Council of Taiwan.

References

[1] Bischoff, B.L. and Anderson, M.A. (1995) Peptization Process in the Sol-Gel Preparation of Porous Anatase TiO_2. *Chemical Materials*, **7**, 1772-1778. http://dx.doi.org/10.1021/cm00058a004

[2] Chrysicopoulou, P., Davazoglou, D., Trapalis, C. and Kordas, G. (1998) Optical Properties of Very Thin (<100 nm) Sol-Gel TiO_2 Films. *Thin Solid Films*, **323**, 188-193. http://dx.doi.org/10.1016/S0040-6090(97)01018-3

[3] Dibble, L.A. and Raupp, G.B. (1992) Fluidized-Bed Photocatalytic Oxidation of Trichloroethylene in Contaminated Airstreams. *Environmental Science and Technology*, **26**, 492-495. http://dx.doi.org/10.1021/es00027a006

[4] Cojocaru, B., Neatu, S., Parvulescu, V.I., Somoghi, V., Petrea, N., Epure, G., Alvaro, M. and Garcia, H. (2009) Synergism of Activated Carbon and Undoped and Nitrogen-Doped TiO_2 in the Photocatalytic Degradation of the Chemical Warfare Agents. *ChemSusChem*, **2**, 427-436. http://dx.doi.org/10.1002/cssc.200800246

[5] Arabatzis, I.M., Stergiopoulos, T., Bernard, M.C., Labou, D., Neophytides, S.G. and Falaras, P. (2003) Silver-Modified Titanium Dioxide Thin Films for Efficient Photodegradation of Methyl Orange. *Applied Catalysis B*: *Environmental*, **42**, 187-201. http://dx.doi.org/10.1016/S0926-3373(02)00233-3

[6] Aruna, S.T., Tirosh, S. and Zaban, A. (2000) Nanosize Rutile Titania Particle Synthesis via a Hydrothermal Method without Mineralizers. *Journal of Materials Chemistry*, **10**, 2388-2391. http://dx.doi.org/10.1039/b001718n

[7] Asahi, R., Morikawa, T., Ohwaki, T., Aoki, K. and Taga, Y. (2001) Visible-Light Photocatalysis in Nitrogen-Doped

Titanium Oxides. *Science*, **293**, 269-271. http://dx.doi.org/10.1126/science.1061051

[8] Babapour, A., Akhavan, O., Azimirad, R. and Moshfegh, A.Z. (2006) Physical Characteristics of Heat-Treated Nano-Silvers Dispersed in Sol-Gel Silica Matrix. *Nanotechnology*, **17**, 763-771. http://dx.doi.org/10.1088/0957-4484/17/3/025

[9] Balek, V., Li, D., Subrt, J., Vecerníková, E., Hishita, S., Mitsuhashi, T. and Haneda, H. (2007) Characterization of Nitrogen and Fluorine Co-Doped Titaniaphotocatalyst: Effect of Temperature on Microstructure and Surface Activity Properties. *Journal of Physical Chemistry and Solids*, **68**, 770-774. http://dx.doi.org/10.1016/j.jpcs.2007.01.028

[10] Carp, O., Huisman, C.L. and Reller, A. (2004) Photoinduced Reactivity of Titanium Dioxide. *Progress in Solid State Chemistry*, **32**, 33-177. http://dx.doi.org/10.1016/j.progsolidstchem.2004.08.001

[11] Li, C.H., Hsieh, Y.H., Chiu, W.T., Liu, C.C. and Kao, C.L. (2007) Study on Preparation and Photocatalytic Performance of Ag/TiO_2 and Pt/TiO_2 Photocatalysts. *Separation and Purification Technology*, **58**, 148-151. http://dx.doi.org/10.1016/j.seppur.2007.07.013

[12] Li, F.B. and Li, X.Z. (2002) Photocatalytic Properties of Gold/Gold Ion-Modified Titanium Dioxide for Wastewater Treatment. *Applied Catalysis A*: *General*, **228**, 15-27. http://dx.doi.org/10.1016/S0926-860X(01)00953-X

[13] Li, F.B. and Li, X.Z. (2002) The Enhancement of Photodegradation Efficiency Using Pt/TiO_2 Catalyst. *Chemosphere*, **48**, 1103-1111. http://dx.doi.org/10.1016/S0045-6535(02)00201-1

[14] Li, J., Xu, J., Dai, W.L., Li, H. and Fan, K. (2009) Direct Hydro-Alcohol Thermal Synthesis of Special Core-Shell Structured Fe-Doped Titania Microspheres with Extended Visible Light Response and Enhanced Photoactivity. *Applied Catalysis B*: *Environmental*, **85**, 162-170. http://dx.doi.org/10.1016/j.apcatb.2008.07.008

[15] Haruta, M. (2007) Size- and Support-Dependency in the Catalysis of Gold. *Catalysis Today*, **36**, 153-166. http://dx.doi.org/10.1016/S0920-5861(96)00208-8

[16] Hashimoto, K., Irie, H. and Fujishima, A. (2005) TiO_2 Photocatalysis: A Historical Overview and Future Prospects. *Japanese Journal of Applied Physics*, **44**, 8269-8278. http://dx.doi.org/10.1143/JJAP.44.8269

[17] Hirakawa, T. and Kamat, P.V. (2005) Charge Separation and Catalytic Activity of Ag@TiO_2 Core-Shell Composite Clusters under UV-Irradiation. *Journal of American Chemical Society*, **127**, 3928-3934. http://dx.doi.org/10.1021/ja042925a

[18] Hirakawa, T. and Kanat, P.V. (2004) Photoinduced Electron Storage and Surface Plasmon Modulation in Ag@TiO_2 Clusters. *Langmuir*, **20**, 5645-5647. http://dx.doi.org/10.1021/la048874c

[19] Hu, C., Hao, Z., Wong, P.K. and Yu, J.C. (2003) Photocatalytic Degradation of Triazine-Containing Azo Dyes in Aqueous TiO_2 Suspensions. *Applied Catalysis B*: *Environmental*, **42**, 47-55. http://dx.doi.org/10.1016/S0926-3373(02)00214-X

[20] Yu, J.C., Yu, J., Yip, H., Wong, P.K., Zhao, J. and Ho, W. (2005) Efficient Visible-Light-Induced Photocatalytic Disinfection on Sulfur-Doped Nanocrystalline Titania. *Environmental Science and Technology*, **39**, 1175-1179. http://dx.doi.org/10.1021/es035374h

[21] Zhang, R. and Gao, L. (2002) Preparation of Nanosized Titania by Hydrolysis of Alkoxide Titanium in Micelles. *Materials Research Bulletin*, **37**, 1659-1666. http://dx.doi.org/10.1016/S0025-5408(02)00817-6

[22] Behar, D. and Rabani, J. (2006) Kinetics of Hydrogen Production upon Reduction of Aqueous TiO_2 Nanoparticles Catalyzed by Pd^0, Pt^0, or Au^0 Coatings and an Unusual Hydrogen Abstraction; Steady State and Pulse Radiolysis Study. *Journal of Physical Chemistry B*, **110**, 8750-8755. http://dx.doi.org/10.1021/jp060971m

[23] Kim, C.S., Moon, B.K., Park, J.H. and Son, S.M. (2003) Synthesis of Nanocrystalline TiO_2 in Toluene by a Solvothermal Route. *Journal of Crystal Growth*, **254**, 405-410. http://dx.doi.org/10.1016/S0022-0248(03)01185-0

[24] Kim, S.B. and Hong, S.C. (2002) Kinetic Study for Photocatalytic Degradation of Volatile Organic Compounds in Air Using Thin Film TiO_2 Photocatalyst. *Applied Catalysis B*: *Environmental*, **35**, 305-315. http://dx.doi.org/10.1016/S0926-3373(01)00274-0

[25] Kim, S.K., Choi, W. and Hwang, S.J. (2005) Visible Light Active Platinum-Ion-Doped TiO_2 Photocatalyst. *Journal of Physical Chemistry B*, **109**, 24260-24267. http://dx.doi.org/10.1021/jp055278y

[26] Pastoriza-Santos, I., Mamedov, A.A., Giersig, M., Kotov, N.A., Liz-Marzán, L.M. and Koktysh, D.S. (2000) One-Pot Synthesis of Ag@TiO_2 Core-Shell Nanoparticles and Their Layer-by-Layer Assembly. *Langmuir*, **16**, 2731-2735. http://dx.doi.org/10.1021/la991212g

[27] Chan, S.C. and Barteau, M.A. (2005) Preparation of Highly Uniform Ag/TiO_2 and Au/TiO_2 Supported Nanoparticle Catalysts by Photodeposition. *Langmuir*, **21**, 5588-5595. http://dx.doi.org/10.1021/la046887k

[28] Wang, W., Zhang, J., Chen, F., He, D. and Anpo, M. (2008) Preparation and Photocatalytic Properties of Fe^{3+}-Doped Ag@TiO_2 Core-Shell Nanoparticles. *Journal of Colloid and Interfacial Science*, **323**, 182-186. http://dx.doi.org/10.1016/j.jcis.2008.03.043

[29] Chuang, H.Y. and Chen, H. (2009) Fabrication and Photocatalytic Activities in Visible and UV Light Regions of Ag@TiO_2 and NiAg@TiO_2 Nanoparticles. *Nanotechnology*, **20**, Article ID: 105704. http://dx.doi.org/10.1088/0957-4484/20/10/105704

[30] Jia, H., Xu, H., Hu, Y., Tang, Y. and Zhang, L. (2007) TiO_2@CdS Core-Shell Nanorods Films: Fabrication and Ramatically Enhanced Photoelectrochemical Properties. *Electrochemical Communications*, **9**, 354-360. http://dx.doi.org/10.1016/j.elecom.2006.10.010

[31] Li, X.Y., Yue, P.L. and Kutal, C. (2003) Synthesis and Photocatalytic Oxidation Properties of Iron Doped Titanium Dioxide Nanosemiconductor Particles. *New Journal of Chemistry*, **27**, 1264-1269. http://dx.doi.org/10.1039/b301998e

[32] Sakai, H., Kanda, T., Shibata, H., Ohkubo, T. and Abe, M. (2006) Preparation of Highly Dispersed Core/Shell-Type Titania Nanocapsules Containing a Single Ag Nanoparticle. *Journal of American Chemical Society*, **128**, 4944-4945. http://dx.doi.org/10.1021/ja058083c

[33] Tom, R.T., Nair, A.S., Singh, N., Aslam, N., Nagendra, C.L., Philip, R., Vijayamohanan, K. and Pradeep, T. (2003) Freely Dispersible Au@TiO_2, Au@ZrO_2, Ag@TiO_2, and Ag@ZrO_2 Core-Shell Nanoparticles: One-Step Synthesis, Characterization, Spectroscopy, and Optical Limiting Properties. *Langmuir*, **19**, 3439-3445. http://dx.doi.org/10.1021/la0266435

[34] Galindo, C., Jacques, P. and Kalt, A. (2001) Photooxidation of the Phenylazonaphthol AO20 on TiO_2: Kinetic and Mechanistic Investigations. *Chemosphere*, **45**, 997-1005. http://dx.doi.org/10.1016/S0045-6535(01)00118-7

[35] Rauf, M.A. and Ashraf, S.S. (2009) Fundamental Principles and Application of Heterogeneous Photocatalytic Degradation of Dyes in Solution. *Chemical Engineering Journal*, **151**, 10-18. http://dx.doi.org/10.1016/j.cej.2009.02.026

[36] Lin, Y.C. and Lin, C.H. (2008) Catalytic and Photocatalytic Degradation of Ozone via Utilization of Controllable Nano-Ag Modified on TiO_2. *Environmental Progress*, **27**, 496-502. http://dx.doi.org/10.1002/ep.10305

[37] Moulder, J.F., Stickle, W.F., Sobol, P.E. and Bomben, K.E. (1995) Handbook of X-Ray Photoelectron Spectroscopy. Physical Electronics.

[38] Li, X.Z., Li, F.B., Yang, C.L. and Ge, W.K. (2001) Photocatalytic Activity of WO_x-TiO_2 under Visible Light Irradiation. *Journal of Photochemistry and Photobiology A*: *Chemistry*, **141**, 209-217. http://dx.doi.org/10.1016/S1010-6030(01)00446-4

[39] Linsebigler, A.L., Lu, G. and Yates Jr., J.T. (1995) Photocatalysis on TiO_2 Surfaces: Principles, Mechanisms, and Selected Results. *Chemical Review*, **95**, 735-758. http://dx.doi.org/10.1021/cr00035a013

[40] Martin, S.T., Morrison, C.L. and Hoffmann, M.R. (1994) Photochemical Mechanism of Size-Quantized Vanadium-Doped TiO_2 Particles. *Journal of Physical Chemistry*, **98**, 13695-13704. http://dx.doi.org/10.1021/j100102a041

[41] Meichtry, J.M., Rivera, V., Iorio, Y.D., Rodríguez, H.B., Román, E.S., Grela, M. and Litter, M.I. (2009) Photoreduction of Cr(VI) Using Hydroxoaluminiumtricarboxymonoamide Phthalocyanine Adsorbed on TiO_2. *Photochemistry and Photobiological Science*, **8**, 604-612.

[42] Natarajan, C. and Nogami, G. (1996) Cathodicel Ectrodeposition of Nanocrystalline Titanium Dioxide Thin Films. *Journal of Electrochemical Society*, **143**, 1547-1550. http://dx.doi.org/10.1149/1.1836677

[43] O'Regan, B. and Grätzel, M. (1991) A Low-Cost, High-Efficiency Solar Cell Based on Dye-Sensitized Colloidal TiO_2 Films. *Nature*, **353**, 737-740. http://dx.doi.org/10.1038/353737a0

[44] Ohno, T., Akiyoshi, M., Umebayashi, T., Asai, K., Mitsui, T. and Matsumura, M. (2004) Preparation of S-Doped TiO_2 Photocatalysts and Their Photocatalytic Activities under Visible Light. *Applied Catalysis A*: *General*, **265**, 115-121. http://dx.doi.org/10.1016/j.apcata.2004.01.007

[45] Park, H.K., Moon, Y.T., Kim, D.K. and Kim, C.H. (1996) Formation of Monodisperse Spherical TiO_2 Powders by Thermal Hydrolysis of $Ti(SO_4)_2$. *Journal of American Ceramic Society*, **79**, 2727-2732. http://dx.doi.org/10.1111/j.1151-2916.1996.tb09038.x

[46] Poznyak, S.K., Kokorin, A.I. and Kulak, A.I. (1998) Effect of Electron and Hole Acceptors on the Photoelectrochemical Behaviour of Nanocrystalline Microporous TiO_2 Electrodes. *Journal of Electroanalytic Chemistry*, **442**, 99-105.

[47] Pruden, A.L. and Ollis, D.F. (1983) Photoassisted Heterogeneous Catalysis: The Degradation of Trichloroethylene in Water. *Journal of Catalysis*, **82**, 404-417. http://dx.doi.org/10.1016/0021-9517(83)90207-5

[48] Sato, S. (1986) Photocatalytic Activity of NO_x-Doped TiO_2 in the Visible Light Region. *Chemical Physics Letter*, **123**, 126-128. http://dx.doi.org/10.1016/0009-2614(86)87026-9

[49] Sonawane, R.S., Kale, B.B. and Dongare, M.K. (2004) Preparation and Photo-Catalytic Activity of Fe-TiO_2 Thin Films Prepared by Sol-Gel Clip Coating. *Materials Chemistry and Physics*, **85**, 52-57. http://dx.doi.org/10.1016/j.matchemphys.2003.12.007

[50] Sonawane, R.S., Hegde, H.G. and Dongare, M.K. (2003) Preparation of Titanium(IV) Oxide Thin-Film Photocatalyst by Sol-Gel Dip Coating. *Materials Chemistry and Physics*, **77**, 744-750.

http://dx.doi.org/10.1016/S0254-0584(02)00138-4

[51] Vamathevan, V., Tse, H., Amal, R., Low, G. and McEvoy, S. (2001) Effects of Fe^{3+} and Ag^{+} Ions on the Photocatalytic Degradation of Sucrose in Water. *Catalysis Today*, **68**, 201-208. http://dx.doi.org/10.1016/S0920-5861(01)00301-7

[52] Wang, C.Y., Liu, C.Y., Zheng, X., Chen, J. and Shen, T. (1998) The Surface Chemistry of Hybrid Nanometer-Sized Particles I. Photochemical Deposition of Gold on Ultrafine TiO_2 Particles. *Colloids Surfaces A*: *Physicochemical and Engineering Aspects*, **131**, 271-280. http://dx.doi.org/10.1016/S0927-7757(97)00086-1

[53] Wang, J., Zhao, H., Liu, X., Li, X., Xu, P. and Han, X. (2009) Formation of Ag Nanoparticles on Water-Soluble Anatase TiO_2 Clusters and the Activation of Photocatalysis. *Catalysis Communications*, **10**, 1052-1056. http://dx.doi.org/10.1016/j.catcom.2008.12.060

[54] Xu, N., Shi, Z., Fan, Y., Dong, J., Shi, J. and Hu, M.Z.C. (1999) Effects of Particle Size of TiO_2 on Photocatalytic Degradation of Methylene Blue in Aqueous Suspensions. *Industrial Engineering Chemistry Research*, **38**, 373-379. http://dx.doi.org/10.1021/ie980378u

[55] Yildiz, A., Lisesivdin, S.B., Kasap, M. and Mardare, D. (2009) Non-Adiabatic Small Polaron Hopping Conduction in Nb-Doped TiO_2 Thin Film. *Physica B*: *Condensed Matter*, **404**, 1423-1426. http://dx.doi.org/10.1016/j.physb.2008.12.034

[56] Yin, S., Fujishiro, Y., Wu, J., Aki, M. and Sato, T. (2003) Synthesis and Photocatalytic Properties of Fibrous Titania by Solvothermal Reactions. *Journal of Materials Processing Technology*, **137**, 45-48. http://dx.doi.org/10.1016/j.physb.2008.12.034

[57] Zhang, F., Pi, Y., Cui, J., Zhang, X., Guan, N. and Yang, Y. (2007) Unexpected Selective Photocatalytic Reduction of Nitrite to Nitrogen on Silver-Doped Titanium Dioxide. *Journal of Physical Chemistry C*, **111**, 3756-3761. http://dx.doi.org/10.1021/jp067807j

[58] Zhang, H. and Chen, G. (2009) Potent Antibacterial Activities of Ag/TiO_2 Nanocomposite Powders Synthesized by a One-Pot Sol-Gel Method. *Environmental Science and Technology*, **43**, 2905-2910. http://dx.doi.org/10.1021/es803450f

[59] Zhang, T., Oyama, T., Aoshima, A., Hidaka, H., Zhao, J. and Serpone, N. (2001) Photooxidative *N*-Demethylation of Methylene Blue in Aqueous TiO_2 Dispersions under UV Irradiation. *Journal of Photochemistry and Photobiology A*: *Chemistry*, **140**, 163-172. http://dx.doi.org/10.1016/S1010-6030(01)00398-7

[60] Zhao, X.F., Meng, X.F., Zhang, Z.H., Liu, L. and Jia, D.Z. (2004) Preparation and Photocatalytic Activity of Pb-Doped TiO_2 Thin Films. *Journal of Inorganic Materials*, **19**, 140-146.

[61] Dobosz, A. and Sobczyński, A. (2003) The Influence of Silver Additives on Titaniaphotoactivity in the Photooxidation of Phenol. *Water Resources*, **37**, 1489-1496.

[62] Dvoranová, D., Brezová, V., Mazúr, M. and Malati, M.A. (2002) Investigations of Metal-Doped Titanium Dioxide Photocatalysts. *Applied Catalysis B*: *Environmental*, **37**, 91-105. http://dx.doi.org/10.1016/S0926-3373(01)00335-6

[63] Behpour, M., Ghoreishi, S.M. and Razavi, F.S. (2010) Photocatalytic Activity of TiO_2/Ag Nanoparticle on Degradation of Water Pollutions. *Digest Journal of Nanomaterial Biostructures*, **5**, 467-475.